Calibrations of digital aerial cameras

Gabriella BOR*, Gergely LÁSZLÓ*,
* Óbuda University, Alba Regia Technical Faculty, Institute of Geoinformatics, Székesfehérvár, HUNGARY
borgabriella97@gmail.com, laszlo.gergely@amk.uni-obuda.hu

***Abstract*— Aerial photography is one of the most effective sources of information to obtain data and examine the condition of different areas of the earth's surface. Their most important role is in the production of maps, as a fresh source of data is essential for their production. Remote sensing and photogrammetry have become increasingly intertwined to this day. The aim of the paper is to describe the calibration process of digital aerial cameras. Calibration is essential for aerial photography for engineering purposes, as without it we would get inaccurate, error-laden results.**
Three cameras were calibrated, two with an Hasselblad A6D-100c sensor with an R 50 (visible in the visible light range) and one with an IR 50 II lens with an IR (infrared in the range). AgiSoft Metashape software was used to examine the geometric calibration. For radiometric calibration, Hasselblad's Phocus image processing program.
My work is part of a "live" task, as I spend my internship at Envirosense Hungary Kft.

I. DIGITAL PHOTOGRAPHY

Digital photography is performed using digital cameras. The cameras can be divided into two groups, measuring cameras and amateur cameras. Amateur cameras are found in almost every household, although nowadays telephone photography is starting to take their place. Digital measuring cameras can be divided into two groups, ground measuring cameras and aerial measuring cameras. The internal data of the cameras are known. These cameras retain this data permanently, unlike amateur cameras.

But what is internal data? The imaging beam is restored, modeled optically during calibration. The imaging beam is the set of projection rays that create the image. The image is created by central projection on the surface of the digital sensor.

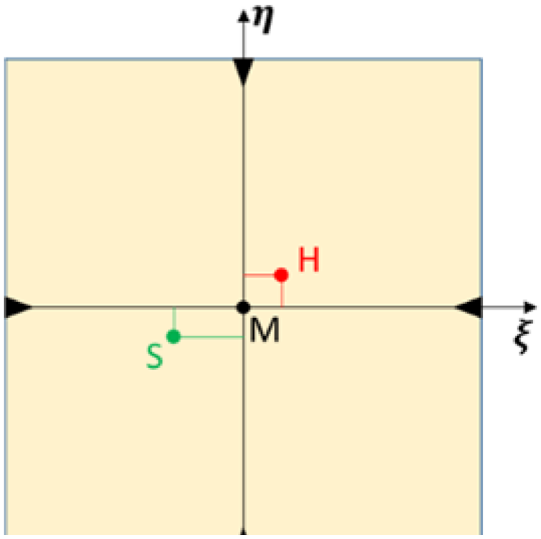

Figure 1. Reference points [1]

H – autocollimation main point
M – center of the image coordinate system
S – center of symmetry
η, ξ - image coordinates of the main point
c_k – camera constant (OH)

These data are determined during the calibration process and can be found in the calibration protocol. If the main point (H) and the center of the image (M) coincide, the camera is aligned. (In the above case, this is not true, apparently does not coincide)

II. AERIAL MEASURING CAMERAS

Parts of aerial measuring cameras [1]:

1. Camera body
2. Negative storage
3. From the cameras

(4.) Other ancillary equipment (GPS, navigation search telescope, overlap control, etc.)

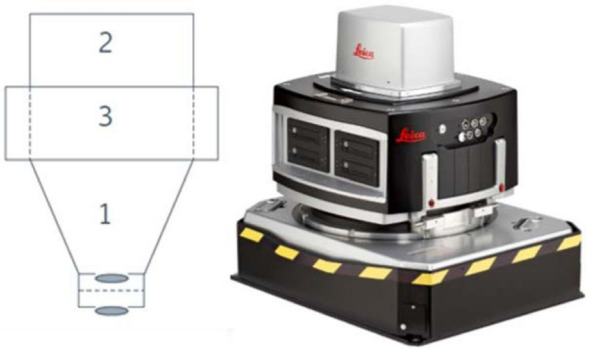

Figure 2. Leica DMC III digital measuring camera [1]

The lens produces the image. The aperture controls how much light it transmits to the sensor. The aperture ring can be used to adjust the gap through which light is allowed in, and to control how much of the incoming light passes through. How long you receive this light is determined by the shutter speed. If light enters through a small aperture, the shutter speed should be increased to allow enough light to reach the negative or the sensor so that the resulting image is not too dark. The settings can be called good if they show a state close to reality. The metering device measures the amount of light on the subject to be photographed. If set to automatic, the appropriate shutter speed and shutter speed will be set. The locking ring is located in the camera body. The aperture affects the depth-of-field range of the image.

Images are formed on a lens system, so in an optical sense, the lens creates the image and this is captured. The point where the camera axis intersects the image plane is called the main point. If the image plane is not perpendicular to the optical axis, the mapping is not ideal. The lens distorts the image. The degree of distortion can be measured. Distortion is the defect of the lens, the distortion resulting from its centering, which increases towards the edge of the image. If light does not arrive on the optical axis, it will be distorted, resulting in a geometric error. The distortion ($\Delta\xi$) is constant over a given radius.

radius (radial) - A_1, A_2, A_3

tangential (perpendicular to the radial) - B_1, B_2

affine - C_1, C_2

Lenses can be grouped according to their viewing angles:

- small $\alpha < 50°$
- medium $50° < \alpha < 60°$
- large $60° < \alpha < 90°$
- very large $90° < \alpha$

The diameter (d) and constant of the objective pupil together are the angle of view (α)

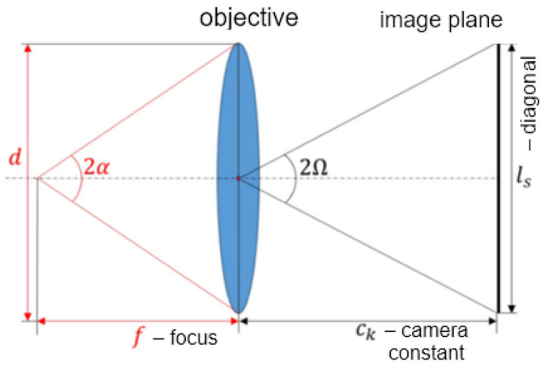

Figure 3. Viewing angles [1]

In the case of the digital image, we speak of surfaces. Digital images are made up of pixels, which are surfaces of extent. We can assign coordinates to a point on the surface. To get these, we need to know the size and extent of the pixels. The pixel coordinate shows how many rows and how many columns a given pixel is in. The higher the number, the finer, more detailed the image. This is characterized by the pixel value. For a camera, how many pixels should be understood as the number of tiny sensor elements located on the surface where the image is captured. In practice, since the number of pixels is in the order of millions, the megapixel unit (mega = 106; million) is used for the number of pixels.

III. Calibrations

The appropriate Hungarian word for calibration is authentication; term related to measuring instruments. In everyday life, scales are calibrated on the market, measuring tapes in geodesy, and all this to get the right, accurate quantity on the measuring instrument. Photogrammetry is associated with the calibration of cameras, measuring cameras and amateur cameras. Camera calibration provides factory data that can be considered authentic, but these are usually checked from time to time to ensure that the nominal data matches the actual data.

One of the purposes of the calibration is to determine the internal data of the camera (η_0, ξ_0, c_k), the other is to eliminate distortion errors by the lens. A camera also requires calibration radiometrically to ensure that the images they take are color-correct.

Calibration can be performed in four ways: In the laboratory, with an control point field, based on asterisks and markers.

A. Camera calibrations in lab

In the laboratory, calibration can be performed in two ways. One option is a rotatable gonimeter, another option is an optical bench rotated at specific angles. For the latter, it is important that the collimators are accurately attached to each other.

In the case of a goniometer, the binoculars (T_1, T_2) must be reset and the glass plate placed in the image plane of the camera, and then the camera is placed in the appropriate position on the turntable, satisfying several aspects. Care should be taken to ensure that the center of the camera's incoming pupil falls on the axis of rotation, this will allow us to detect the crosshairs of the telescope in the mirror image. At the same time, the main point H can be determined.

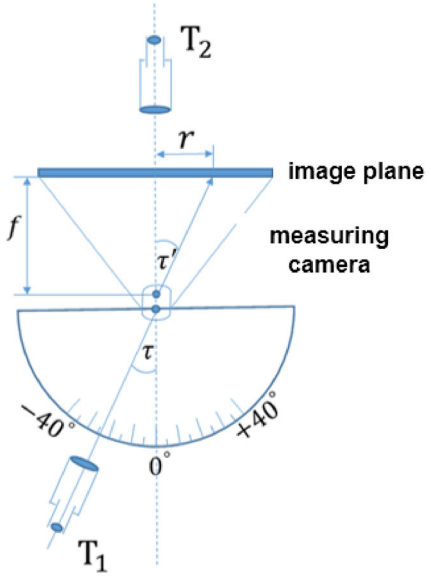

Figure 4. Camera calibration in the laboratory [1]

During the measurement, the τ -angles are measured, so the difference between the angles of the autocollimation main point (H) and the directed grid points is formed. To reduce the errors resulting from the measurement result, we calculate the plotting values and construct their curves, for which first a middle curve and then a smoothing line can be edited. This gives the distortion values.

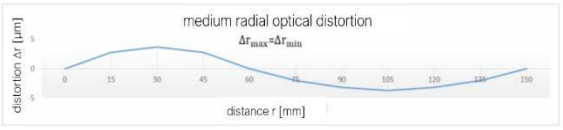

Figure 5. Medium radial optical distortion [1]

B. Camera calibrations with control point field

Field points should be marked, so that they are evenly distributed and have a depth difference of at least twenty percent of the average shooting distances. The coordinates of the control points can be considered known (X_i, Y_i, Z_i)) and are ideal if they can be measured on at least two recordings (ξ_i, η_i)

Relationship between image and object coordinates:

$$\xi = \xi_0 - Ck\frac{r_{11}(x-x_0)+r_{21}(y-y_0)+r_{31}(z-z_0)}{r_{13}(x-x_0)+r_{23}(y-y_0)+r_{33}(z-z_0)} + \Delta x$$

$$\eta = \eta_0 - Ck\frac{r_{12}(x-x_0)+r_{22}(y-y_0)+r_{32}(z-z_0)}{r_{13}(x-x_0)+r_{23}(y-y_0)+r_{33}(z-z_0)} + \Delta y$$

The collination equation is modified by Δx, Δy, considering the optical plot and the affine distortion of the sensor. These corrections can be grouped as radial plot (A_1, A_2, A_3), tangential plot (B_1, B_2), and affine distortion (C_1, C_2) parameters.

Radial distortion:

$$\Delta r_{rad} = A_1 \cdot r^3 + A_2 \cdot r^5 + A_3 \cdot r^7$$

r: the distance of a given pixel from the main point

$$r = \sqrt{(\xi - \xi_0)^2 + (\eta - \eta_0)^2}$$

$$\Delta x_{rad} = (\xi - \xi_0) \cdot \frac{\Delta r_{rad}}{r}$$

$$\Delta y_{rad} = (\eta - \eta_0) \cdot \frac{\Delta r_{rad}}{r}$$

Tangential distortion:

$$\Delta x_{tan} = B_1 \cdot (r^2 + 2 \cdot (\xi - \xi_0)^2) + 2 \cdot B_2 \cdot (\xi - \xi_0) \cdot (\eta - \eta_0)$$

$$\Delta y_{tan} = B_2 \cdot (r^2 + 2 \cdot (\eta - \eta_0)^2) + 2 \cdot B_2 \cdot (\xi - \xi_0) \cdot (\eta - \eta_0)$$

Calculating the unknowns: The control point field is created, evenly distributed, which can be measured with a geodetic instrument. The values of η and ξ are derived from the measurement.

1. Installation and measurement of control points → $X_i; Y_i;\ Z_i$

2. Take at least three shots

3. Measurement of alignment points (ξ; η) on the recordings

4. Determining the preliminary value of unknowns

5. Perform equalization with gradual approximation

a) $Adx + l = v$ system of correction equations

b) $A^T A dx + A^T l = A^T v \rightarrow N \cdot dx + n = 0$

c) $dx = -N^{-1} - n$

d) $dx + x^{(0)} = x^{(1)} \rightarrow dx^{(1)} + x^{(1)} = x^{(2)} \leftarrow$ *gradual approximation*

6. Error calculation

$$\sigma_0 = \frac{\sqrt{\sum Ni}}{\mathrm{f}}$$

$$f = n - u$$

$$\sigma_n = \sigma_0\sqrt{qnn}$$

C. Camera calibration based on stars

When we calibrate our camera based on stars, the field's control points are replaced by the stars. For the calibration to be successful, the position of the images relative to the celestial coordinate system must be known and the image coordinates (ξ, η) of the photographed stars must be measured. If image coordinate corrections and camera internal data are used, the relationship between the sky and image coordinate system can be written.

$$\begin{bmatrix} X \\ Y \\ Z \end{bmatrix} = K \cdot \begin{bmatrix} cos\alpha \cdot cos\delta \\ sin\alpha \cdot cos\delta \\ sin\delta \end{bmatrix} = K \cdot \begin{bmatrix} U \\ V \\ W \end{bmatrix} \qquad R\begin{bmatrix} \xi - \xi_0 - \Delta x \\ \eta - \eta_0 - \Delta y \\ -c_k \end{bmatrix}\begin{bmatrix} U \\ V \\ W \end{bmatrix}$$

$$K = \sqrt{(\xi - \xi_0 - \Delta x)^2 + (\eta - \eta_0 - \Delta y)^2 + c_k^2}$$

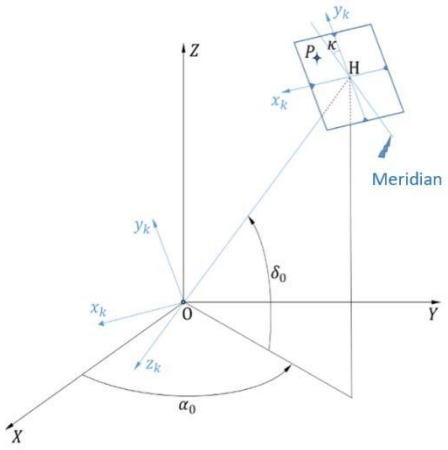

Figure 6. Camera calibration based on stars [1]

ξ, η – image coordinates of points
c_k, ξ_0, η_0 – camera internal data
Δx, Δy – image coordinate corrections
O – projection center
H – main point
α – right ascension
δ – declination angles
K – pixel vector length

$$(\xi - \xi_0) \cdot (1 - A_1 \cdot r^2 - A_2 \cdot r^4 - A_3 \cdot r^6 = -c_k \cdot \frac{r_{11} \cdot U + r_{21} \cdot V + r_{31} \cdot W}{r_{13} \cdot U + r_{23} \cdot V + r_{33} \cdot W}$$

$$(\eta - \eta_0) \cdot (1 - A_1 \cdot r^2 - A_2 \cdot r^4 - A_3 \cdot r^6 = -c_k \cdot \frac{r_{12} \cdot U + r_{22} \cdot V + r_{32} \cdot W}{r_{13} \cdot U + r_{23} \cdot V + r_{33} \cdot W}$$

To be able to calibrate by stars, a minimum of five stars must be measured. Atmospheric refraction significantly affects the recordings - it is important to eliminate this during processing - therefore photography in the zenith direction is recommended because the effect of refraction is small there. As with other different measurements, it is advisable to record the measurement data (e.g. exact time, temperature, air pressure, camera setting data, etc.). Using various astronomical programs, the precession, nutation, motion, daily and annual aberration of the star can be calculated, and then the exact coordinates of these values can be calculated from these values, with the knowledge of which the calibration can be performed.

D. Camera calibration with coded signals

In this calibration procedure, the test diagrams act as control points. Images should be taken with a fixed focus value and calibration should be performed with the same focus value. It is a good idea to take shots from multiple points of view, thus increasing reliability when the points in the test area are in one plane. During the measurement, images were taken from three positions where the cameras were rotated in the plane of the sensor. The cameras we examined consist of a Hasselblad A6D-100c sensor and an HC 50 II lens, medium format cameras. In terms of resolution, 100 megapixels. Its sensor surface is 53.4 × 40.0 mm, where the image is created. In general, for digital cameras, the size of the medium format sensors is 43.8 × 32.9 mm and 53.7 × 40.2 mm. By geometric resolution we mean the size of the smallest image unit captured by a sensor that actually corresponds. This is better the lower its value. This type contains 11600 × 8700 sensors.

Figure 7. HC 50 II lens

They can be classified as medium format cameras that use a film size of 120 or use a digital imaging sensor that produces this size 120. This format produces slightly smaller images than large format films (102x127 mm), but larger than images taken with full-frame sensors or 135 films. There are no standard sizes, they usually vary from manufacturer to manufacturer. Another feature of medium format cameras is that they capture outstandingly high quality images and also provide high accuracy in terms of color accuracy. In addition, they are larger and heavier than most cameras due to the large sensors. Its great advantage is that it is modular, ie its components can be replaced according to your own needs.

Figure 8. Hasselblad A6D-100c

IV. Description of the test

The measurement was performed on the ground floor of the Institute, in front of the Council Hall. Due to the size of the site and the black and white flooring, it was ideal for the task. Fifty-two control points were selected that covered the test area. 16 markers were glued to the wall opposite the cameras and the rest were placed away from the cameras and placed there. The remaining signs were placed on both sides of the wall, to door openings, and to pegs set up in the middle of the area. We made sure that most of the points were visible from all three positions. Four images were taken from one position, rotating the camera clockwise by 90 ° in the plane, i.e., a total of twelve images were taken with one camera. The points were also measured with a measuring station. The markers used in the study could be downloaded depending on the software.

Figure 9. Markers

RGB and NIR cameras were calibrated in Agisoft. Each image was checked separately. Because we used the program's own punctuation marks, the software was able to recognize them automatically. We checked to see if there were any markers in the image that look good and that they were in the right place. The algorithm was not flawless, where markers did not show the entire surface, there it did not recognize them, and there was one of the markers reflected on the glass that confused it. The partially visible points where the signal center was well identifiable were marked manually. There were times when only after calibration, the results showed (the example below) that a point had been identified, they were in the wrong place. After running the repair and calibration again, the correct values have been reached.

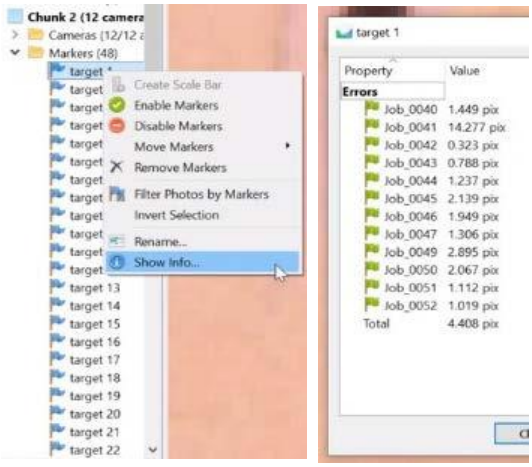

Figure 10. Extent of inconsistencies in pixels per signal and per image

Figure 11. Location of markers

Larger defects were typically at points closer to the camera. They were faulty not only because the distance changed from more distant points, but also because they were not sharply formed, they were blurred because of their proximity.

We obtained the fixed focus, the coordinates of the main image point, the parameters of three radial plots and two tangential plots, the metric size of the sensor surface.)

The following results show the error of the X, Y, Z components, expressed in meters for RGB and IR cameras:

#Label	X	Y	Z	Error_(m)	X_error	Y_error	Z_error
target 1	21,352	-0,177	1,236	0,006549	0,001648	-0,006012	-0,002007
target 2	21,234	-1,387	1,224	0,006018	0,002323	-0,005526	-0,000529
target 3	21,101	-2,778	1,27	0,005879	0,001453	-0,005623	-0,000913
target 4	21,006	-3,855	1,25	0,003525	-0,001949	-0,002865	0,000646
target 5	21,351	-0,218	0,594	0,006276	0,000921	-0,006204	-0,000208
target 6	21,236	-1,411	0,568	0,005094	0,001313	-0,004922	0,000019
target 7	21,107	-2,788	0,552	0,003232	-0,00017	-0,003218	-0,000244
target 8	21,009	-3,882	0,551	0,003647	-0,000183	-0,003632	-0,000275
target 9	21,348	-0,185	-0,452	0,005748	-0,000054	-0,005747	0,000093
target 10	21,227	-1,503	-0,404	0,005869	-0,000832	-0,005769	0,000682
#Total Error				0,007268	0,003156	0,006428	0,001242

#Label	X	Y	Z	Error_(m)	X_error	Y_error	Z_error
target 1	21,352	-0,177	1,236	0,006255	0,001745	-0,00572	-0,00184
target 2	21,234	-1,387	1,224	0,005401	-0,00025	-0,00534	-0,00076
target 3	21,101	-2,778	1,27	0,006107	-0,00075	-0,0059	-0,0014
target 4	21,006	-3,855	1,25	0,005127	0,002141	-0,00452	0,001142
target 5	21,351	-0,218	0,594	0,005949	0,000446	-0,00593	-0,0001
target 6	21,236	-1,411	0,568	0,004887	-0,00112	-0,00476	-0,00017
target 7	21,107	-2,788	0,552	0,00348	0,000017	-0,00347	-0,00031
target 8	21,009	-3,882	0,551	0,00408	0,00005	-0,00408	-0,00018
target 9	21,348	-0,185	-0,452	0,00545	0,000397	-0,00544	-0,000063
target 10	21,227	-1,503	-0,404	0,006174	-0,00263	-0,00556	0,000577
#Total Error				0,006648	0,002556	0,006044	0,001061

Figure 12. RGB, IR camera results

Because of clarity, of the 52 points, I illustrate only the first ten measurements per camera, as these were the points that appeared from almost every position without exception. In the bottom row, the mean error values are to be interpreted for all points.

	Value	Error	F	Cx	Cy	B1	B2	K1	K2	K3	K4	P1	P2
F	10860.8	27.9465	1.00	0.04	-0.21	-0.39	-0.02	-0.99	0.97	-0.94	0.88	0.05	-0.17
Cx	1.67084	5.57294		1.00	-0.02	0.00	0.33	-0.04	0.04	-0.04	0.04	0.98	-0.01
Cy	-83.665	6.25971			1.00	0.32	-0.04	0.20	-0.18	0.17	-0.15	-0.02	0.99
B1	0.288139	1.39263				1.00	-0.01	0.40	-0.38	0.33	-0.27	0.01	0.34
B2	-2.22266	0.533042					1.00	0.02	-0.03	0.03	-0.03	-0.34	-0.04
K1	0.0813215	0.0406388						1.00	-0.99	0.97	0.92	-0.05	0.16
K2	-0.467382	0.241445							1.00	-0.99	0.96	0.05	-0.15
K3	1.44	0.646567								1.00	-0.99	-0.05	0.13
K4	-1.77949	0.663881									1.00	0.05	-0.11
P1	-0.000140808	0.000274598										1.00	0.00
P2	-0.00318663	0.000306481											1.00

Figure 13. Distortion matrix

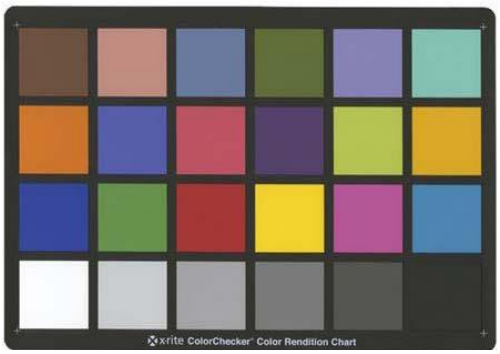

Figure 14. Color calibration table

For radiometric correction, a color calibration table was used, which was imaged at Papkutapuszta Airport. The closer we take pictures of it, the easier it will be for Phocus to recognize the board, but the focal length had to be taken into account.

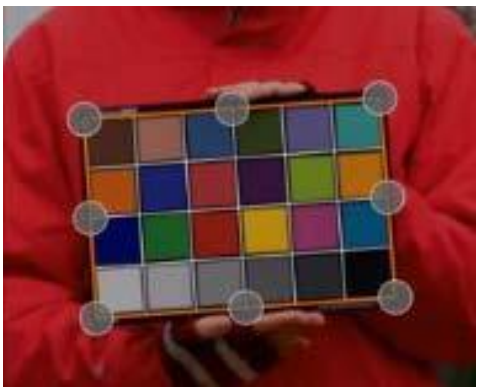

ΔE avg.: 1.73 max.: 3.94

ΔE avg.: 1.82 max.: 4.47

The recorded images were calibrated in Hasselblad's Phocus image processing program. In the *Color Calibratio*n menu, *Auto Locate* - which automatically recognizes the color scheme - did not work because it did not recognize the target, meaning you had to manually attach the grid to the color calibration board. Then, by clicking on *Calibrate*, he calibrated the image and calculated the ΔE values shown above and as a result we obtained the radiometrically corrected images. The visual difference between ΔE two colors, which can take a value between 0 and 100, in our case the average value below 2 should be interpreted so that the deviation from the reference can only be noticed by a very experienced eye on a monitor calibrated to a better value. Detection of the difference below 1 is only possible with a target instrument test. In the

description of the figures, the maximum value is around 4, which is already a visible difference for some colors. Strangely, the biggest difference is in black in both cases. [2]

V. Sensor types

A. CCD and CCD

CCD and CMOS are the best known digital image capture modes. On the surface of these sensors, the photosensitive elements are arranged in a linear or matrix manner. The CCD (Charge Coupled Device) is considered the first digital camera. The chip transmits the incoming light in front of the lens as a digital signal to another device that can be read and processed. The result will be an image of near-perfect quality, with minimal distortion, even at low light requirements. One of the disadvantages is that the manufacturing cost of the CCD chip is very high, in contrast to CMOS. The other downside is that it gets very hot due to high energy consumption, so the thermal noise will also be higher. CMOS (Complementary Metal-Oxide-Semiconductor) is considered the "little brother" of CCD. It uses a photoelectric effect in the same way as its "big brother". The camera uses less power to extend its life. It is more sensitive to electromagnetic interference than the CCD.

Where should the image capture happen? Obviously where my optically produced image is sharp. The optical law of sharp imaging determines where the image is sharp. A sharp image is obtained if the reciprocal of the focal length (f) is equal to the sum of the reciprocal of the subject distance (t) and the reciprocal of the image distance (k).

$$\frac{1}{f} = \frac{1}{t} + \frac{1}{k}$$

B. Multispectral cameras

Digital multispectral satellite remote sensing systems are based on multispectral cameras. Multispectral sensors are those that are able to capture electromagnetic energy in several wavelength ranges. It is possible to display the image for data recorded in different spectral ranges. The simultaneous visual representation of combinations of these data is called composite. As a result, the recordings can be studied thoroughly, as data can be discovered on them that the human eye alone cannot perceive.

C. LIDAR

LIDAR (Light Detection and Ranging), which can be classified as active systems, measures reflected electromagnetic energy in the visible, infrared and ultraviolet ranges. The recorded data does not depend on the humidity and shade of the air, so it does not depend on the weather or the time of day.

D. RGB sensors

Sensors that detect three ranges of visible light and have different spectral sensitivities are located next to each other. The spectral ranges of these sensors are as follows:

R (red)	650 nm – 750 nm
G (green)	490 nm – 575 nm
B (blue)	420 nm – 490 nm

We see these colors in the pictures the same way we see them with the naked eye.

E. NIR sensors

The infrared range can be divided into three parts, near, medium and far infrared. Our camera is able to capture images in the near-infrared wavelength range from 760 nm to 900 nm, on which field objects appear in false colors.

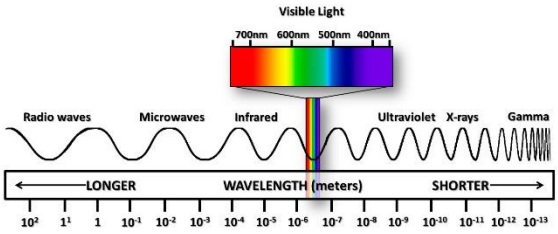

Figure 15. Electromagnetic spectrum ranges [3]

VI. Softwares which was used for calibration

Agisoft

Agisoft is one of the best known point cloud software. The program automatically detects the points in the test field, then measures and assigns the numbers. This is possible because, according to a geometric arrangement, the markers are unique, carry code in themselves, or because the coded signals complement the grid or markers of the test field and recognize their orientation. [5]

Phocus

Hasselblad's image processing software is Phocus, which works with all Hasselblad cameras, but can of course be used for photos taken with any camera. [6]

VII. DIGITAL ORTHOPHOTO PRODUCTION

The cameras examined in my dissertation are used to produce digital orthophotos. Orthophoto is a special photo transformation that is free from distortion. There are two types of distortion. One is perspective distortion due to the fact that the image plane is not parallel to the object plane. The other is altitude distortion, which is caused by elevation differences in the terrain.

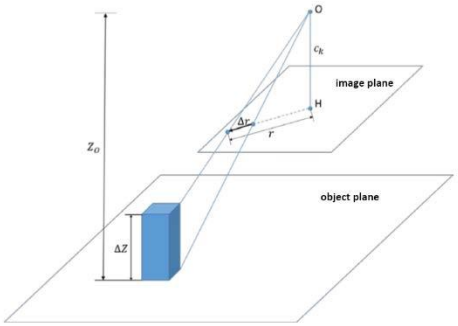

Figure 16. Δr distortion [1]

Δz: that can be extracted from the topography model

r: distance of point from nadir

$$\Delta r = \Delta z \cdot \frac{r}{c_k \cdot M_k} \qquad M_k = \frac{h_k}{c_k}$$

Two types of digital elevation models (DMM) are known. The digital terrain model (DDM) and the digital terrain model / surface model (DTM / DFM0).

If only topography is depicted, then we are talking about a traditional orthophoto, if "everything is in place" (buildings, vegetation, etc.), then we are talking about a real orthophoto.

Before taking an orthophoto, we need to know how accurate the terrain model is.

For the terrain model, how inaccurate it can be, i.e. the allowable error, can be calculated as follows:

$$mz_{max} = \frac{\Delta r \cdot C_{K \cdot m_0}}{r}$$

Orthophoto production process:

Step 1: Data Preparation

- original image: in digital or analogue form and scanning
- image orientation
  elements of internal information (c_k, ξ_0, η_0)
  elements of external information $(X_0, Y_0, Z_0, \varphi, \omega, \kappa)$
- digital elevation model: acquisition or production
  if we produce: based on contour maps contour lines; by field measurement; aerial laser scanning (LIDAR); possible by photogrammetry, which requires a pair of stereo images.

Step 2: Select an orthophoto area

- enter corner coordinates (usually EOV);
- we adjust the orthophoto to the resolution of our original image

Rule 1: The resolution of the orthophoto is always better than the original image

Rule 2: Up to twice as good

Step 3: The required values must be assigned to the orthophoto pixels

$$0 \leq g_i \leq 255$$

Basic equation of central projection:

$$\xi = -C_k \frac{r_{11}(x - x_0) + r_{21}(y - y_0) + r_{31}(z - z_0)}{r_{13}(x - x_0) + r_{23}(y - y_0) + r_{33}(z - z_0)}$$

$$\eta = -C_k \frac{r_{12}(x - x_0) + r_{22}(y - y_0) + r_{32}(z - z_0)}{r_{13}(x - x_0) + r_{23}(y - y_0) + r_{33}(z - z_0)}$$

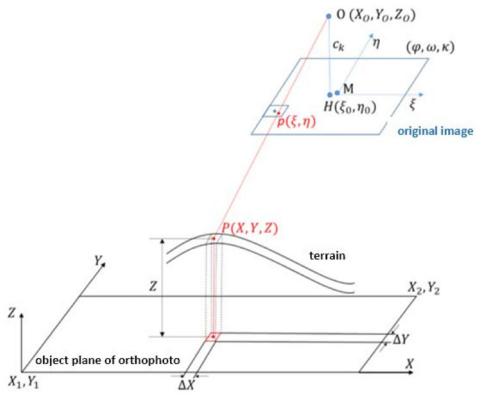

Figure 17. Digital orthophoto production [1]

1. The principle of immediate neighborhood
2. Bilinear interpretation
(4g value eg 1 | weighted average)

$$g' = \frac{\sum g_i \cdot s_i}{\sum s_i}$$

3. Tertiary collination
   - For 4 × 4 pixel cubes
   - The contrast of the image decreases in the orthophoto, ie the image "becomes lifeless", therefore it is recommended to contrast enhancement

4. Making an orthophoto mosaic
   - Marking the cutting edges and joining them along it
   - Several orthophotos cover an area
   - Rule 1: along lines (road, rail, land border)
   - Rule 2: Lines should be cut perpendicularly
   - color balance is required for matching

5. Orthophoto map alignment
   - Scale, projection, coordinate, mapping writings (north direction, coupon number, scale, etc. writing)
   - Directly suitable for mapping

VIII. Summary

The purpose of this article was to describe the calibration process of digital aerial cameras. We calibrated three cameras, two RGB (visible in the visible light range) and one IR (infrared in the range) Hasselblad A6D-100c sensor, equipped with an HC 50 II lens, which is owned by Envirosense Hungary Kft.

Calibration of the cameras is essential to produce a high-precision end product.

The test shows why calibration should be performed in all cases. In theory, the cameras we examined should arrive at the customer with appropriate calibration values for both the goods and their category, however, the distortion diagrams show that the distortion is significant even when moving towards the edges of the lenses. Which might not be a big problem with ground-based photogrammetry, but for aerial photography at 2,000 meters above the surface, the errors can be so significant that it makes it difficult to perform aerial triangulation of flights designed primarily with less overlap. This is because the software we use (Trimble OrthoVista) is a specifically rigid-wing mainframe, so it expects high-precision data as input, so if the distortion at the image edges exceeds a certain level, the automatic alignment search algorithm will not find a match within those error limits. points, so the number of areas with multiple overlaps will also be significantly reduced, which will also negatively affect ultimate accuracy. In addition, there may be a problem in making orthomosaics that while the accuracy on the inside of the images is good, after constructing the boundaries, the final product does not appear to have been composed of different images; already clearly shows that the geometric accuracy is not uniform within the images.

In addition to the numerical accuracy, the real, visible results of the calibrations presented in the dissertation will be revealed during the flights to be performed in the near future.

In the future I will also cover these results, and I will try to further improve the geometric accuracy with the help of BINGO software and possibly other calibration procedures.

IX. References

[1] Dr. habil Jancsó Tamás: Digitális fotogrammetria jegyzet (2017)

[2] Delta E 101 by Zachary Schuessler http://zschuessler.github.io/DeltaE/learn/?fbclid=IwAR1WxtC7JeEb72rV0Db1Qpz6o-hp2uNAqMlKGzOWDe7Sc2sbeubeORNX3zQ

[3] Verőné Wojtaszek Malgorzata: Fotointerpretáció és távérzékelés: A távérzékelés fizikai alapjai (2011)

[4] Bácsatyai László: Magyarországi vetületek (2005)

[5] Agisoft Metashape Manual: https://www.agisoft.com/pdf/metashape-pro_1_5_en.pdf

[6] Phocus by Hasselblad Manual http://static.hasselblad.com/2014/12/Phocus-User-Manual_v14_-ENG_2016.pdf

[7] Katona, Janos ; Gulyas, Margit Horoszne Determination of factors modifying land value based on spatial data
In: Drótos, Dániel; Vásárhelyi, József; Czap, László; Ivo, Petráš (szerk.)
Proceedings of the 19th International Carpathian Control Conference (ICCC 2018)
Piscataway (NJ), Amerikai Egyesült Államok : IEEE, (2018) pp. 625-628.

[8] Alhusain, Othman ; Tóth, Zoltán ; Rakusz, Ádám ; Almási, László ; Farkas, Bertalan Vision-based System for Quality Control of Some Food Products ISPRS JOURNAL OF PHOTOGRAMMETRY AND REMOTE SENSING XXXV pp. 477-482. , 6 p. (2004) Nyilvános idézők összesen: 3 Független: 3 Függő: 0

[9] Barsi, Árpád ; Fi, István ; Mélykúti, Gábor ; Lovas, Tamás ; Tóth, Zoltán Úthibák detektálása - Mobil felmérő rendszer fejlesztése a BME-n MÉLYÉPÍTŐ TÜKÖRKÉP: A SZAKMA LAPJA

2005 : 2 pp. 32-33. , 2 p. (2005) Matarka Zárolt Nyilvános idézők összesen: 3 Független: 0 Függő: 3

[10] Tóth, Zoltán ; Mélykúti, Gábor ; Barsi, Árpád Digitális videokamera kalibrációja GEOMATIKAI KÖZLEMÉNYEK / PUBLICATIONS IN GEOMATICS 8 pp. 297-302. , 6 p. (2005) Folyóiratcikk/Szakcikk (Folyóiratcikk)/Tudományos